Available online at www.sciencedirect.com

SciVerse ScienceDirect

Ceramics International 39 (2013) 7217–7222

CERAMICS INTERNATIONAL

www.elsevier.com/locate/ceramint

Short communication

Dryout temperature–vapor pressure profile of polymeric fiber containing refractory castables

Rafael Salomão[a,*], Victor C. Pandolfelli[b]

[a]*Materials Engineering Department, São Carlos School of Engineering, University of São Paulo, Avenida Trabalhador São-carlense 400, 13560–970, São Carlos, SP, Brazil*

[b]*Materials Engineering Department, Federal University of São Carlos, Rodovia Washington Luís km 235, São Carlos, SP, Brazil*

Received 6 December 2012; received in revised form 7 January 2013; accepted 8 January 2013
Available online 16 January 2013

Abstract

Different types of polymeric fibers are added to refractory castables' formulations as drying additives to make dewatering processes easier and reduce the risks of explosive spalling of these low permeability materials. Many works describe how these fibers control the permeability increase in castables before and after their melting-decomposition. The water vapor pressure profile developed inside the structure and how it is modified by the fiber presence has not yet been explored systemically. In the present paper, thin K-type thermocouples were inserted (at different depths) in polymeric fibers (olefin copolymer, polypropylene and aramidic ones) containing castable samples. Their temperature profile and mass loss were recorded during the first heat-up. After combining internal heating and mass loss rate, vapor pressure levels calculated using Antoine's equation, hot air permeametry (HAP) and work of fracture (γ_{WOF}) results, novel insights into the mechanisms by which polymeric fibers avoid explosive spalling during castables dewatering were attained.

Keywords: A. Drying; E. Refractories; Fibers

1. Introduction

A refractory castable's first heat-up process is a complex operation [1–4]. Due to its high packing density, water vapor entrapment can lead to cracking or even explosions. Therefore, information associated to the amount of remaining water and the vapor pressure developed inside castable structures during water withdrawal can be a powerful tool to prevent explosions and design safer and less time consuming drying schedules. Besides that, their low permeability and thermal conductivity does not allow dewatering to be carried out in a single step [5–7].

Different physicochemical phenomena occur depending on the temperature range, atmospheric conditions (temperature and humidity) and water content in the structure. Based on these aspects, the drying behavior of cement containing castables can be divided into three main sequential stages which, under continuous heating, can be clearly identified by thermogravimetry (Fig. 1) [6–8]. The drying rate is usually calculated using the derivative of the W_D (wt%) parameter, which represents the cumulative fraction of water released during the heat-up, according to the expressions:

$$W_D = 100\% \times (M_0 - M)\,/(M_F) \quad (1)$$

$$(\mathrm{d}W_D/\mathrm{d}t)_i = (W_{Di+10} - W_{Di-10})/(t_{i+10} - t_{i-10}) \quad (2)$$

where M is the instantaneous mass recorded at time t_i during the heating stages of the samples, M_0 is the initial mass and M_F is the final one. At the beginning of the drying, water is withdrawn by evaporation and low drying rates and vapor pressure levels are attained (Fig. 1a(i)). (2) Afterwards, during ebullition (from 100 °C up to 250–300 °C (Fig. 1a(ii)), the water vapor pressure (P_{Vapor}) shows an exponential increase with the inner temperature (this behavior is described by Antoine's Equation, as follows) and significantly higher drying rates are observed. (3) Finally, in the dehydroxilation or dehydration steps,

*Corresponding author. Tel.: +55 16 33739576; fax: +55 16 33739590.
E-mail addresses: rsalomao@sc.usp.br, rflslm@gmail.com (R. Salomão), vicpando@ufscar.br (V.C. Pandolfelli).

0272-8842/$ - see front matter
http://dx.doi.org/10.1016/j.ceramint.2013.01.018

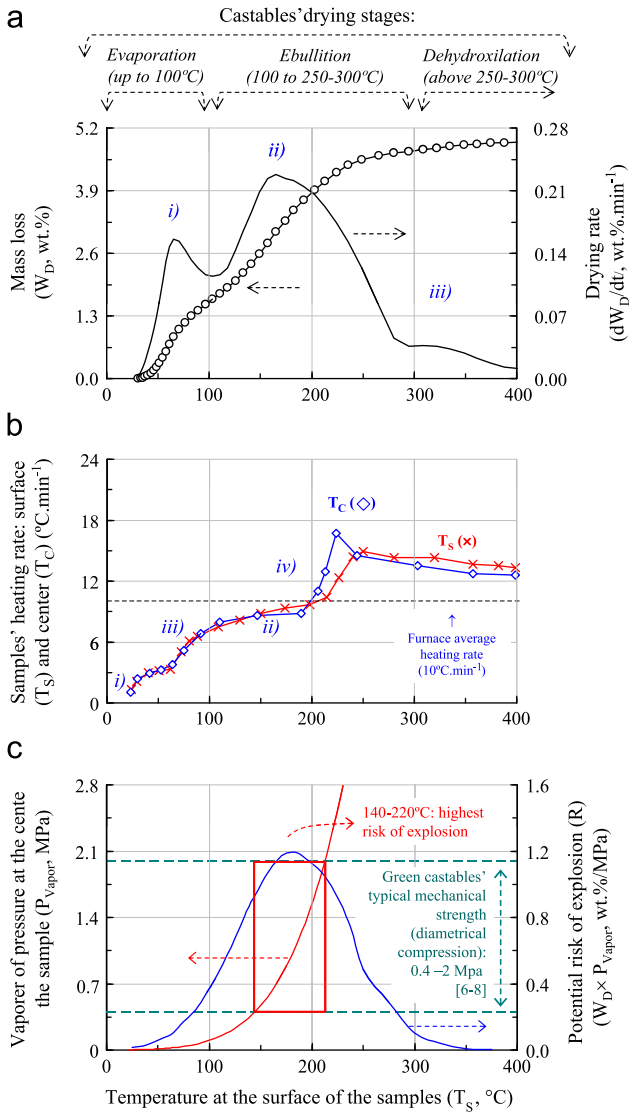

Fig. 1. Typical drying behavior of a self-flowing refractory castable followed by (a) thermogravimetry and (b) inner temperature measurements. (c) The potential risk of explosions (R parameter, Eq. (5)) was estimated combining the water vapor pressure (P_{Vapor}) values calculated using Antoine's Eq. (3), the W_D results and the typical values of mechanical strength for green castable [6–8].

hydrated compounds (such as calcium aluminate cement hydrates are decomposed, Fig. 1a(iii).

Mass loss and vapor pressure data recording, nevertheless, presents various experimental difficulties. Due to their large and variable sizes, continuous castable weighting during the first heat-up step is not an easy task. The connections between pressure transducers and the inside of the material are rarely leakage-free, also making the in-situ vapor pressure measurements not quite feasible. Besides this, the transducers themselves could behave as a critical defect reducing the mechanical strength and favoring the spalling. Alternatively, these difficulties were overcome using an indirect approach based on monitoring castables' surfaces and inner temperatures using a previously inserted thermocouple cast at different material depths [7,8]. Having these temperature profiles and the correspondent changes at the heating rates, important information can be attained.

Because water vaporization is a first-order transformation with a high latent heat, more energy is spent to heat H_2O than the solid castable particles. For that reason, during vapor release, the heating rate measured inside the castable is significantly lower than the one attained based on the furnace inputs (Fig. 1b(i) and (ii). As a consequence, sudden heating rate increases can be observed at the end of each drying stage (Fig. 1(iii) and (iv)). Therefore, this heating rate recording can be used to control the length and define the end of each drying stage.

Additionally, the role of temperature on water vapor pressure can be described by Antoine's equation:

$$P_{Vapor} = \mathrm{EXP}[A - (B/(T_C + C))] \quad (3)$$

where, P_{vapor} (MPa) is the water vapor pressure at a certain temperature at the center of the sample (T_C, in Kelvin degrees) and, A, B and C are empirical dimensionless constants ($A = 23.224$, $B = 3841.22$ and $C = -45.0$) [7,8]. This equation is particularly useful to predict water vapor pressure in closed vessels containing liquid water and vapor and its validity is from 100 °C up to 340 °C. In this range, water vapor pressure varies exponentially with the temperature (Fig. 1c), whereas other variables, such as humidity and concentration gradients, play minor roles. This information can be combined with the thermogravimetric results (Fig. 1a) and applied to monitor and control the vapor pressure profiles attained during the dewatering process. Based on typical values of green castable mechanical strength (Fig. 1c), the vapor pressure (P_{Vapor}) levels calculated using Antoine's Eq. (3) at the center of the sample (T_C) and on the amount of free-water remaining in the structure at the same particular time (W_D, Eq. (1), Fig. 1a), the pressurization risk (R, expressed in wt% MPa) can be estimated and used to evaluate the safety of different heating rates (Fig. 1c) [6–8]:

$$R_i = W_{Di} \times P_{Vapori} = 100\% \times (M_0 - M_i)/(M_F) \times \mathrm{EXP}(A - B/(T_{Ci} + C)) \quad (4)$$

In the present work, the R function was used to evaluate the effect of different polymeric fibers on castable drying behavior. Olefin copolymer (OC), Polypropylene (PP) and polyaramid (PAr) fibers are well known for their suitable performance as drying additives for refractory castables [9–13]. Previous publications described the mechanisms by which these types of fibers induce a controlled permeability [14–16] and work of fracture [17,18] increase in castables and the various fiber composition and geometry requirements necessary to make the drying process effective. These results, however, were not yet related to the water vapor pressure profile developed inside the castable and how it is modified by the fibers. For a high-alumina castable formulation, the calculated vapor pressure levels and the potential risk of explosion results attained were compared to mass loss rate profiles, hot air permeametry (HAP)

results (previously reported in the literature [11,12,19,20]) and the thermal characterization of the fibers Fig. 2.

2. Experimental

The self-flow refractory castable formulation selected was designed according to Andreasen's particle packing model (coefficient $q=0.21$ and free-flow index = 100%). The raw materials comprised a mix of fine matrix powders (24 wt%, $D_{Part} < 100$ μm, A1000SG and E-sy 1000, Almatis, US) and coarse white fused alumina aggregates (76 wt%, $D_{Part\ Max}=4750$ μm, Elfusa Geral de Eletrofusão, Brazil), 2 wt% of calcium aluminate cement (ca.270, Almatis, Germany). 4.12 wt% (15 vol%) of water was added for mixing and cement hydration. Three different types of thin polymeric fibers were dry mixed with the formulation in a volumetric amount of 0.36% (Table 1).

After mixing, compositions were cast vertically in cylindrical molds (40 mm × 40 mm) for the drying and heating rate tests. During casting, thin k-type thermocouples were inserted just below the surface and at the center of the samples, at half-height of the cylinder (Fig. 2). The curing of the samples was performed at 10 °C, in an acclimatized chamber (Vötsch 2020), under an atmosphere with ≈100% relative humidity for 15 days. This condition was used to enhance the effects of the low permeability on castables' dryout [2,22,23].

The drying tests were performed using a thermogravimetric apparatus which can simultaneously record at 1-second intervals of the mass variations and temperature

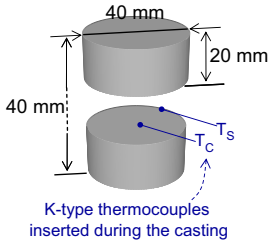

Fig. 2. Thin k-type thermocouples (Ø ~ 0.3 mm) were inserted in the samples used for drying and temperature measurement tests. All the results are presented as a function of the temperature at the surface of the samples (T_S); the temperature at the center of the samples (T_C) was used for the water vapor pressure calculations.

profile inside the furnace and at the sample's surface and center, under a heating rate of 10 °C min^{-1}, from 20 °C to 400 °C [6–8].

The heating rates at the surface and center of the samples were calculated using the following equation:

$$(dT_X/\mathrm{d}t)i = (T_{Xi+10} - T_{Xi-10})/(t_{i+10} - t_{i-10})s \quad (5)$$

where, T_{Xi} is the instantaneous temperature at the surface (T_S) or center (T_C) of the sample recorded at different t_i times during the heating stages.

The hot air permeametry (HAP) technique uses a pre-heated air flow at high constant pressure (0.3 MPa), which is forced to percolate a previously dried 26 mm thickness × 70 mm diameter sample [11,12]. Under this condition, this air flow becomes highly sensitive to changes in its path throughout the porous medium. Due to this, any permeability increase triggered by heating (such as polymeric fibers melting) is revealed as an air flow rate enhancement. HAP results are presented as air flow rate versus temperature curves. Detailed description of the equipment used and the technique can be found in previous publications by the authors [11–13,21], as for the work of fracture measurements [17,18].

3. Results and discussion

After mixing and during casting, the polymeric fibers are scattered as tri-dimensional nets, throughout the castables' structure [10]. Depending on the fiber melting and decomposition temperatures and their thermomechanical strength, different effects can be observed in the castables' drying behavior. Due to this, the results attained are presented in two sections, as follows, based on these different aspects.

3.1. Permeability increase based on the fiber chemical nature: olefin copolymer (OC) and polypropylene (PP)

Because OC and PP are thermoplastic materials, these fibers melt and decompose during the first heating, generating highly permeable paths (Fig. 3a). These paths connect themselves, pores, permeable matrix-aggregates interfaces and the surface of the material [12–14], increasing the drying rate and shortening the drying time (Fig. 3b)

Table 1
Typical characteristics of the polymeric fibers tested.

Fibers	Olefin copolymer (OC)	Polypropylene (PP)	Aramidic (PAr)
Amount added to the castables (vol%) (wt%)	0.36 [0.09]	0.36 [0.1]	0.36 [0.06]
Density (g cm^{-3}) (Ref. [19–21])	0.88 ± 0.05	0.95 ± 0.05	1,47 ± 0.08
Diameter (μm) (Ref. [15–16])	15 ± 1	15 ± 1	20 ± 2
Nominal length (mm) (Ref. [15–16])	6 ± 0.5	6 ± 0.5	6 ± 0.5
Melting point (°C) (Ref. [19–21])*	75–100	165-220	–
Decomposition (°C) (Ref. [19–21])*	100–250	220–380	395–518
Loss of 10 % of the initial elastic modulus (°C) (Ref. [17,18])*	–	120	320

*Using synthetic air atmosphere and heating rate of 10 °C/min.

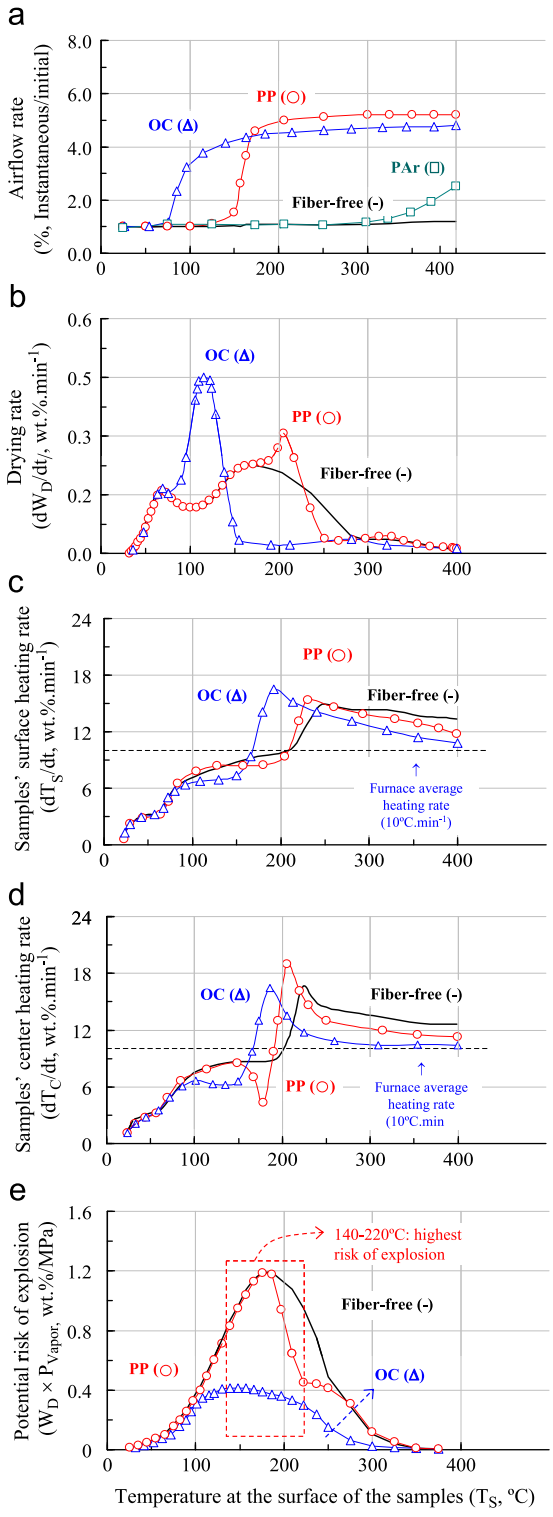

Fig. 3. Refractory castables samples containing olefin copolymer (OC) and polypropylene (PP) fibers: (a) hot air permeametry (HAP) [12,19–21]; (b) drying rate profile; heating rate profile at the (c) surface and (d) center of the samples; (e) potential risks of explosive spalling.

[12,21]. As pointed out by other work in the literature, the lower the melting temperature of the fibers, the earlier the permeability increase and the greater the benefits on the drying rate [19–21].

Regarding the temperature profiles, compared to the fiber-free composition, significantly lower heating rates at the surfaces and at the centers of the samples (Fig. 3c and d) can be observed during the ebullition stage. This effect indicates that the high permeability of these structures allowed more energy to be spent vaporizing water, preventing its pressurization. It can also be noted that the earlier finish of the ebullition stage (Fig. 3b) was followed by a sudden increase in the surface and center heating rates (Fig. 3c and Fig. 3d, respectively). In this case, the high permeability generated by the fibers resulted in a more efficient water withdrawal, shortening the drying stages [12,21].

Considering the combined effects of the vapor pressure development (calculated using temperature measurements carried out in the center of the samples, T_C) and the amount of water which remained inside the structure at a certain moment (W_D), it can be observed that OC and PP fiber additions also significantly reduced the risks of explosive spalling (the R function, Fig. 3e) above 130 °C and 170 °C, respectively, by two related ways: (a) the permeability increase inhibited the structure overheating, reducing T_C mean values and (b) faster dewatering reduced the amount of water in the structure during the critical temperature interval and, therefore, the amount of vapor formed.

3.2. Work of fracture (γ_{WOF}) effect: aramidic fibers (PAr)

Polyaramid fibers present high mechanical strength which are used in bullet-proof and aerospace composites, and for high temperatures (up to 250–300 °C) applications [17–20]. Various articles report that an addition of 0.36 vol% of these fibers prevented the explosive spalling of a self-flowing castable in a condition at which the fiber-free reference failed [17–18]. Combining these results previously reported in literature [17] and those present in Figs. 3a and 4b–e, it can be pointed out that these fibers behave differently from the OC and PP ones.

The PAr fibers can increase castables' permeability up to a level equivalent to the one attained with the PP ones (Fig. 4a) after a thermal treatment at 900 °C [19,20]. However, because the permeability increase only occurs above 320 °C (Fig. 3a), no significant changes were observed at the drying rate (Fig. 4b) or temperature (Fig. 4c and d) profiles. Therefore, in this case, the anti-spalling mechanism can be attributed to the outstanding thermo-mechanical properties of the polyaramid fibers and to their enhanced castables work of fracture (γ_{WOF}) (Fig. 4a) [17,18] in the temperature range at which the spalling risks are high (140–220 °C, Fig. 4e).

4. Final remarks

Monitoring the inner temperature and water vapor pressure built-up profile during the refractory castables' drying step provided novel insights regarding the

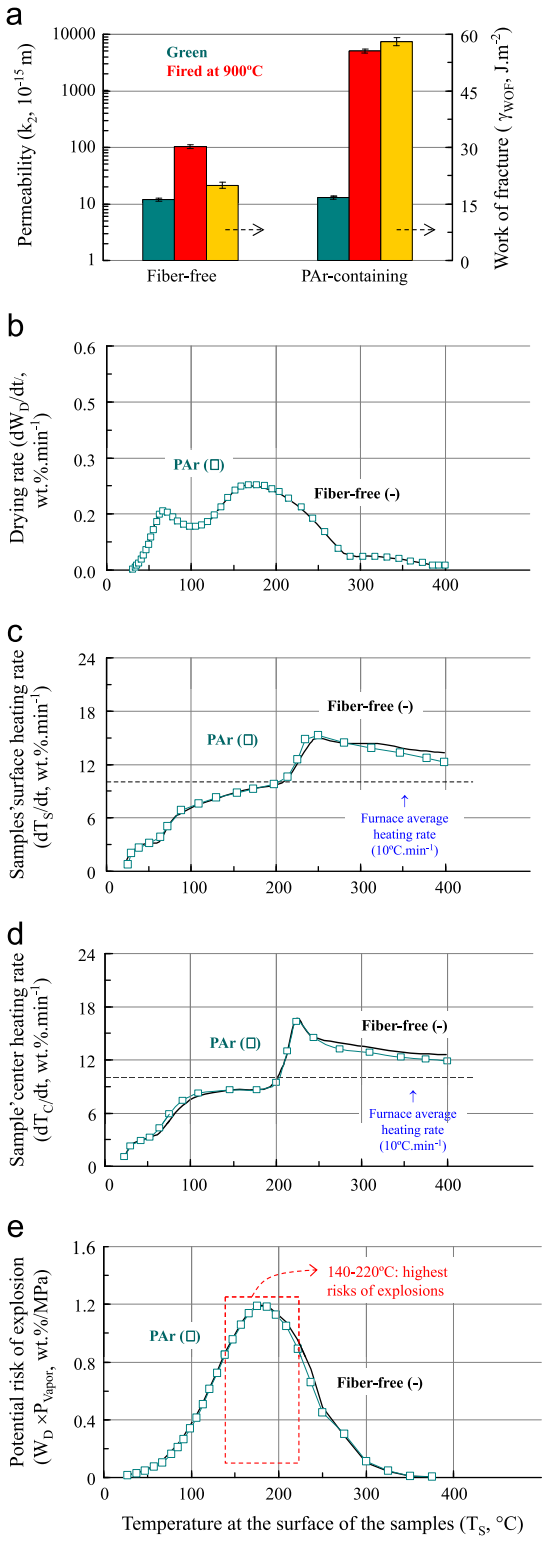

Fig. 4. Refractory castables samples containing aramidic (PAr) fibers: (a) work of fracture of the green castable (after drying at 110 °C) [17,18]; (b) drying rate profile; heating rate profile at the (c) surface and (d) center of the samples; (e) potential risks of explosive spalling.

mechanisms by which polymeric fibers behave as drying additives. The permeability increase generated by the thermoplastic fibers (olefin copolymer, OC, and polypropylene, PP) during their melting and decomposition, enhanced samples' drying rate, shortened the whole process and also modified the heating rate and vapor pressure built-up from the samples. Significantly lower heating rates at the surface and at the center of these samples were observed indicating that water vaporization towards the surface was favored instead of its pressurization inside the structure. Combining the water vapor pressure (P_{Vapor}) calculated using Antoine's equation and the drying rate (W_D) results showed that the potential risk of explosion (the R function) was significantly reduced. Comparing the performance of the PP and OC fibers pointed out that the OC ones were more effective as a drying additive because: (a) they prevented structure overheating via an earlier permeability increase, reducing the mean temperature of the inner layers of the material and (b) they allowed much faster dewatering, reducing the amount of water in the structure during the critical temperature interval and, therefore, the amount of vapor formed. For the aramidic fibers (PAr) containing samples, on the other hand, no significant changes to the drying rate, heating rate or pressure built-up profiles were observed. Therefore, the anti-spalling mechanism described in the literature based on work of fracture enhancement was confirmed. Finally, it is reasonable to consider that the combination of both classes of fibers would result in even safer and easy-drying materials.

Acknowledgments

We thank Brazilian Research Funding agencies FAPESP and CNPq, FIRE and Magnesita Refratários S.A. for supporting this work.

References

[1] W.H. Gitzen, L.D. Hart, Explosive spalling of refractory castables bonded with calcium aluminate cement, American Ceramic Society Bulletin 40 (8) (1961) 503–510.
[2] M.S. Crowley, R.C. Johnson, Guidelines for installing refractory concrete linings in cold weather, American Ceramic Society Bulletin 51 (2) (1972) 171–176.
[3] W.E. Lee, R.E. Moore, Evolution of in situ refractories in the 20th century, Journal of American Ceramic Society 81 (6) (1998) 1385–1410.
[4] R.E. Moore, J.D. Smith, W.L. HeadrickJr., T.P. Sander, Monolithic dewatering theory testing and practice: new challenges, in: Proceedings of the 32th Annual Symposium on Refractories, The American Ceramic Society, St. Louis, 1996, pp. 1–19.
[5] G. Scherer, Theory of drying, Journal of American Ceramic Society 73 (1) (1990) 3–14.
[6] M.D.M. Innocentini, F.A. Cardoso, M.M. Akiyoshi, V.C. Pandolfelli, Drying stages during heating of high-alumina, ultra-low-cement refractory castables, Journal of American Ceramic Society 86 (7) (2003) 1146–1148.
[7] M.D.M. Innocentini, M.F. Miranda, F.A. Cardoso, V.C. Pandolfelli, Vaporization process and pressure buildup during dewatering of dense refractory castables, Journal of American Ceramic Society 86 (9) (2003) 1500–1503.
[8] M.D.M. Innocentini, F.A. Cardoso, A.E.M. Paiva, V.C. Pandolfelli, Dewatering refractory castables, American Ceramic Society Bulletin 83 (7) (2004) 9101–9108.

[9] P.H. Havranek, Recent developments in abrasion- and explosion-resistance castables, American Ceramic Society Bulletin 62 (2) (1983) 234–243.
[10] D.P. Bentz, Fibers, percolation and spalling of high-performance concrete, American Concrete Institute Materials Journal 97 (3) (2000) 351–359.
[11] M.D.M. Innocentini, C. Ribeiro, R. Salomão, L.R.M. Bittencourt, V.C. Pandolfelli, Assessment of mass loss and permeability changes during the dewatering process of refractory castables containing polypropylene fibers, Journal of American Ceramic Society 85 (8) (2002) 2110–2112.
[12] R. Salomão, V.C. Pandolfelli, Drying behavior of polymeric fiber-containing refractory castables, Journal of the Technical Association of Refractories(Japan) 24 (2) (2004) 83–87.
[13] R. Salomão, V.C. Pandolfelli, The PSD effect on the drying efficiency of polymeric fibers containing castables, Ceramics International 34 (2008) 173–180.
[14] R. Salomão, F.A. Cardoso, M.D.M. Innocentini, L.R.M. Bittencourt, V.C. Pandolfelli, Effect of polymeric fibers on refractory castable permeability, American Ceramic Society Bulletin 82 (4) (2003) 51–56.
[15] R. Salomão, A.M. Zambon, V.C. Pandolfelli, Polymeric fiber geometry affects refractory castables permeability, American Ceramic Society Bulletin 85 (4) (2006) 9201–9205.
[16] R. Salomão, V.C. Pandolfelli, Polypropylene fibers and their effects on processing refractory castables, International Journal of Applied Ceramic Technology 4 (2007) 496–502.
[17] C.M. Peret, V.C. Pandolfelli, Steel fibers and the mechanical behavior of refractory castables on drying, American Ceramic Society Bulletin 85 (1) (2006) 9401–9407.
[18] C.M. Peret, P. Bonadia, M. Brito, V.C. Pandolfelli, The dry out profile of steel micro-fiber containing refractory castables, Refractories Applications 15 (2010) 10–13.
[19] M.D.M Innocentini, R. Salomão, C. Ribeiro, F.A. Cardoso, R. Rettore, L.R.M. Bittencourt, V.C. Pandolfelli, Permeability of fiber-containing refractory castables—part I, American Ceramic Society Bulletin 81 (7) (2002) 34–38.
[20] M.D.M Innocentini, R. Salomão, C. Ribeiro, F.A. Cardoso, R. Rettore, L.R.M. Bittencourt, V.C. Pandolfelli, Permeability of fiber-containing refractory castables—part II, American Ceramic Society Bulletin 81 (8) (2002) 65–68.
[21] R. Salomão, L.R.M. Bittencourt, V.C. Pandolfelli, High-performance drying additives for refractory castables: engineered polymeric fibers, American Ceramic Society Bulletin 87 (2008) 9101–9106.
[22] F.A. Cardoso, M.D.M. Innocentini, M.M. Akiyoshi, L.R.M. Bittencourt, V.C. Pandolfelli, Scale-up effect on the drying behavior of high-alumina refractory castables, Journal of the Technical Association of Refractories (Japan) 23 (4) (2003) 226–230.
[23] M.D.M. Innocentini, A.R. Studart, M.M. Akiyoshi, A.E. Paiva, L.R.M. Bittencourt, V.C. Pandolfelli, The drying behavior of high-alumina ultra-low cement refractory castables under different heating rates, Refractories Applications 7 (5) (2002) 17–20.